Research Square

Preprints are preliminary reports that have not undergone peer review.
They should not be considered conclusive, used to inform clinical practice,
or referenced by the media as validated information.

Existence of both polarity ion-acoustic supersolitons and double layers with wave transition sequence in two temperature non-extensive electron plasma

Somir Ali

somir5660@gmail.com

Bhattadev University

Kamal Saharia

Bhattadev University

Article

Keywords: ion-acoustic waves, supersolitons, double layers, Sagdeev pseudopotential, Two-temperature electrons

Posted Date: November 20th, 2026

DOI: https://doi.org/10.21203/rs.3.rs-11589797/v1

License: This work is licensed under a Creative Commons Attribution 4.0 International License.
Read Full License

Additional Declarations: No competing interests reported.

Existence of both polarity ion-acoustic supersolitons and double layers with wave transition sequence in two temperature non-extensive electron plasma

Somir Ali* **and K. Saharia**

Department of Physics, Bhattadev University, Bajali, Pathsala, 781325, Assam, India

****Corresponding author. E-mail:*** *somir5660@gmail.com*

Abstract

The propagation of electrostatic solitary waves are investigated in a three component collisionless plasma, consisting of fluid positive ions and two temperature non-extensive electrons with their own non-extensive indices. Using the Sagdeev pseudo-potential technique, distinct classes of nonlinear waves are investigated. It is found that the solitons, double layers, and supersolitons of both polarities (compressive and rarefactive) exist in this configuration. A parametric analysis is done to explore how the non-extensivity along with Mach number variation modify the amplitude, width and threshold conditions for emerging the structures. Notably, a distinct wave transition sequence is observed in rarefactive regime, where the nonlinear structures systematically evolve from solitary waves to double layers and then to supersolitons, ultimately transit to a soliton with higher amplitude, i.e., a soliton (before the double layer) $\rightarrow$ double layer $\rightarrow$ supersoliton $\rightarrow$ soliton (after the supersoliton), with increasing non-extensive parameter and Mach number independently. The present investigation may be helpful for the basic characteristic study of nonlinear structures in laboratory as well as astrophysical plasmas.

Key words: ion-acoustic waves; supersolitons; double layers; Sagdeev pseudopotential; Two-temperature electrons

1 Introduction

The study of ion acoustic supersolitons gained increasing attention after Dubinov and Kolotkov [1,2] first reported them in an unmagnetized plasma model comprising five components. However, they later reported the existence of such waves in four component plasmas and suggested that at least four plasma components may be required for the formation of supersolitons when one of the electron populations follows Maxwellian distribution [3]. Before being identified as a distinct class of localized nonlinear structures by Dubinov and Kolotkov, similar wave profiles had already been observed in some earlier studies [4-7], however they were not recognized or categorized as supersolitons. Mathematically, supersolitons can arise when the Sagdeev pseudopotential exhibits three consecutive local extrema between the undisturbed state and an accessible root. This characteristic nonlinear structure is accompanied by a wiggling pattern in the

electric-field profile, while the corresponding phase portrait exhibits oscillatory or wavy features around the separatrix [8-10]. Later, Verheest et al. [11] demonstrated the existence of such structures (supersolitons) in a three component plasma consists of positive ions, negative ions, and non-thermal electrons. Subsequently, many authors, including Baluku et al. [4] studied the existence and characteristics of ion-acoustic positive-potential supersolitons (PPSSs) in an unmagnetized plasma composed of fluid ions and two-temperature electrons following kappa distribution. Singh et al. [12] studied ion acoustic solitary waves viz., positive potential solitary waves (PPSWs), positive potential double layers (PPDLs) and PPSSs formation in an unmagnetized three component plasma containing Cairns-distributed nonthermal hot electrons and cool Maxwellian electrons. X. Mushinzimana et al. [13] have investigated ion acoustic solitary structures viz., PPSWs, PPDLs and PPSSs in a three component plasma comprising positive ions, negative ions and super-thermal kappa distributed electrons. Rufai et al. [14] were the first to report obliquely propagating supersolitons in a magnetized three component plasma within a certain range of plasma parameters and subsequently investigated ion acoustic structures, including negative potential solitary waves (NPSWs), negative potential double layers (NPDLs) and negative potential supersolitons (NPSSs) in a magnetized plasma composed of fluid ions and two temperature electrons featuring a Cairns distribution. D. Debnath et al. [15] investigated ion-acoustic solitary structures in a dusty, collisionless, magnetized three component plasma comprising static dust grains, warm ions and non-thermal electrons, they demonstrated that further variation of the plasma parameters can cause a rarefactive supersoliton to revert to a regular soliton after formation of supersoliton but they did not report for any PPDLs. Paul et al. [16] investigated dust-ion-acoustic waves in a four-component plasma consisting of non-thermal electrons, positrons, warm ions, and static dust (e-p-i-d). They also demonstrated a transition from supersolitons to regular solitons with increasing Mach number but did not report for any NPSSs. One of the pioneering studies on the existence of supersolitons was reported by Lakhina et al. [17], who established that three-component plasmas consisting of two ion species and Boltzmann-distributed electrons cannot support supersolitons. Subsequently, Verheest et al. [18] demonstrated that ion-acoustic supersolitons are also absent in two-component unmagnetized plasmas. These findings indicate that a minimum of three distinct plasma components is required for the formation of supersoliton structures in unmagnetized plasma. The above studies considered two-temperature electron populations with non-Maxwellian velocity distributions, motivated by observational and experimental evidence of non-thermal particle populations in space and laboratory plasmas. Space missions [19-23] have revealed distinct electron populations with different temperatures and significant departures from Maxwellian behavior, while laboratory experiments have likewise confirmed long-tailed, non-Maxwellian electron distributions [24]. In particular, FAST [25,26] and Freja [19] observations provide evidence of energetic electron populations in the auroral and upper-ionospheric regions. To describe these non-Maxwellian electron populations and account for the long range interactions in complex plasma systems, Tsallis [27,28] introduced the framework of non-extensive statistics, characterized by the entropic index q, which recovers to classical Boltzmann–Gibbs statistics in the limit $q \to 1$. The resulting non-extensive distribution has been widely used to investigate nonlinear wave dynamics in space and laboratory plasmas [8,9,29-31].

Shalini and Saini [29] investigated solitons and double layers of both polarities (viz., PPSWs, PPDLs, NPSWs, and NPDLs) using such non-Maxwellian distributions in an unmagnetized plasma composed of non-extensive cold electrons, hot electrons and positive ions. Very recently,

R. Kakoti and K. Saharia [32] investigated PPSWs, PPDLs, and PPSSs in a plasma consisting of fluid positive ions, Maxwellian cold electrons and non-extensive hot electrons. However, a significant gap remains in the literature regarding three component plasma systems. To the best of our knowledge, no existing study has reported solitons, double layers and supersolitons of both polarities within the same unmagnetized plasma model with transition sequence of the waves. The closest exception is the work by S. Dalui et al. [33], where they have successfully demonstrated the existence of PPSSs,PPSWs, NPSWs, NPDLs, and NPSSs along with the transition from NPSSs to NPSWs by varying a single plasma parameter θ only, the angle of propagation with respect to the static magnetic field in a magnetized plasma system with two temperature electrons, but they did not report any PPDLs in their configuration.

In this work, we investigate an unmagnetized, collisionless, three component plasma comprising fluid ions and non-extensive cold and hot electrons to explore various nonlinear structures. Shalini and Saini [29] investigated this plasma configuration and reported compressive and rarefactive solitary waves and double layers only for certain parameter values, but did not report for any supersolitons or wave transition sequence. Here, using the Sagdeev pseudopotential formalism, we systematically investigate the effect of Mach number and non-extensive parameter q on the distinct classes of nonlinear structures. Our analysis reveals both positive and negative potential supersolitons, in addition to conventional solitary waves and double layers and exhibits a transition from supersolitons to regular solitary waves in the rarefactive regime, as confirmed by the corresponding bifurcation diagrams. The associated tripolar electric-field signature further provides a characteristic feature of supersolitons. Overall, the existence of PPSWs, PPDLs, PPSSs, NPSWs, NPDLs, and NPSSs, together with the observed transitional sequence between nonlinear structures, provides a comprehensive description of ion-acoustic nonlinear excitations in an unmagnetized three-component plasma with two-temperature electrons.

This manuscript is arranged as follows: In Sec. 2, the basic equations of our plasma system and the obtained Sagdeev pseudo-potential is discussed. Section 3 is devoted to analyzing the existence of different waves and the associated transitional sequence. Finally, the conclusions are presented in Sec. 4.

2 Theoretical model

We consider an unmagnetized, collisionless plasma consisting of cold inertial singly charged positive ions and two populations of Tsallis-distributed electrons: cold electrons (temperature T_c, density n_c) and hot electrons (temperature T_h, density n_h). At equilibrium, charge neutrality requires $n_{i0} = n_{c0} + n_{h0}$. Defining the cold electron concentration $f = n_{c0}/n_{i0}$, the hot-electron fraction follows as $n_{h0}/n_{i0} = 1 - f$. With these plasma components and their equilibrium conditions, the ion dynamics are described by the normalized continuity and momentum equations, which are coupled with Poisson's equation as [29]:

$$\frac{\partial N}{\partial T} + \frac{\partial (NU)}{\partial X} = 0, \tag{1a}$$

$$\frac{\partial U}{\partial T} + U\frac{\partial U}{\partial X} + \frac{\partial \phi}{\partial X} = 0, \tag{1b}$$

$$\frac{\partial^2 \phi}{\partial X^2} = fN_c + (1-f)N_h - N, \tag{1c}$$

where $N = n_i/n_{i0}$, $U = u_i/C_s$, $\phi = e\Phi/k_B T_{\rm eff}$ are the normalized ion density, ion velocity and electrostatic potential respectively , while X and T are the space and time coordinates normalized by the effective Debye length $\lambda_{Deff} = (k_B T_{\rm eff}/4\pi e^2 n_{i0})^{1/2}$ and the ion plasma period $\omega_{pi}^{-1} = (m_i/4\pi e^2 n_{i0})^{1/2}$ respectively. The effective electron temperature is $T_{\rm eff} = T_c/[f+(1-f)\beta]$, with $\beta = T_c/T_h$ .The Tsallis-distributed cold and hot electron densities, normalized to their equilibrium values are

$$\begin{aligned} N_c &= [1 + (q_c - 1)\phi]^{\frac{q_c+1}{2(q_c-1)}}, \\ N_h &= [1 + \beta(q_h - 1)\phi]^{\frac{q_h+1}{2(q_h-1)}}. \end{aligned} \tag{2}$$

where q_c and q_h are parameters representing strength of non-extensivity of the cold and hot electrons respectively. For the study of arbitrary amplitude nonlinear structures in the plasma, Eqs. (1) are transformed into the wave frame $\zeta = X - MT$, where M is the Mach number normalized to the sound speed and other symbols have their usual meanings. Using the boundary conditions $\phi \to 0$, $N \to 1$, $d\phi/d\zeta \to 0$ as $|\zeta| \to \infty$, the ion continuity and momentum equations integrate to

$$N = \left(1 - \frac{2\phi}{M^2}\right)^{-1/2}, \tag{3}$$

which remains real, and hence physically admissible, only for $M^2 \geq 2\phi$. Substituting Eqs. (2) and (3) into Poisson's equation and integrating with respect to ϕ yields the pseudo-energy balance equation

$$\frac{1}{2}\left(\frac{d\phi}{d\zeta}\right)^2 + V(\phi) = 0, \tag{4}$$

formally identical to the equation of motion of a unit-mass pseudo-particle moving with pseudo-velocity $d\phi/d\zeta$ in the Sagdeev pseudopotential $V(\phi)$, which is derived as:

$$\begin{aligned} V(\phi) = M^2 \left[1 - \sqrt{1 - \frac{2\phi}{M^2}}\right] + \frac{2f}{3q_c - 1}\left[1 - (1 + (q_c - 1)\phi)^{\frac{3q_c-1}{2(q_c-1)}}\right] \\ + \frac{2(1-f)}{(3q_h - 1)\beta}\left[1 - (1 + \beta(q_h - 1)\phi)^{\frac{3q_h-1}{2(q_h-1)}}\right]. \end{aligned} \tag{5}$$

Here the three terms represent the inertial ion contribution and the pressure like contributions of the nonextensive cold and hot electrons respectively. This pseudopotential becomes identical to that reported in the Ref. [32] when the cold electrons are considered Maxwellian ($q_c \to 1$). The nature of the nonlinear electrostatic solitary structures admitted by Eq. (5) is fixed by the standard Sagdeev potential conditions given below:

1. **Soliton:** $V(0) = V'(0) = 0$, and $V''(0) < 0$. $V(\phi_m) = 0$ with $V(\phi) < 0$ for $0 < |\phi| < |\phi_m|$.
2. **Double layer:** $V(\phi_{DL}) = V'(\phi_{DL}) = 0$, and $V''(\phi_{DL}) < 0$, with $V(\phi) < 0$ for $0 < |\phi| < |\phi_{DL}|$.
3. **Supersoliton:** Beyond $|\phi_{DL}|$, $V(\phi)$ develops an extra local extremum while $V(\phi) < 0$ throughout, satisfying $V(\phi_s) = 0$ for $|\phi_s| > |\phi_{DL}|$.

The polarity of the solitary structures is positive (compressive) for $\phi > 0$ and negative (rarefactive) for $\phi < 0$. The threshold Mach number can be obtained from Eq. (5) by imposing the

condition $V''(0) \leq 0$, which yields

$$M_{\min} = \left[\frac{2}{f(q_c+1)+(1-f)\beta(q_h+1)}\right]^{1/2}. \tag{6}$$

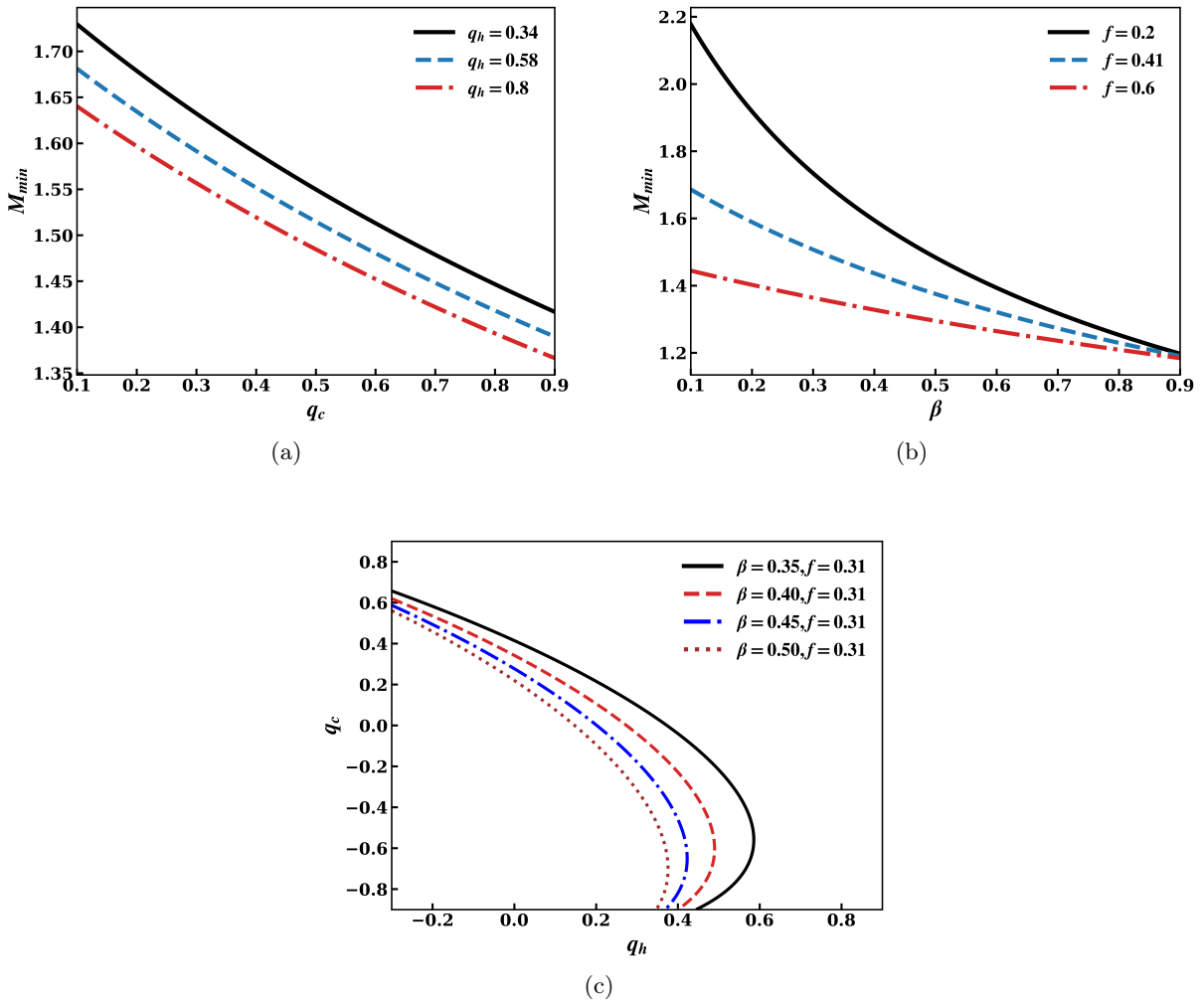


Figure 1: (a) $M_{\min}$ as a function of q_c for different q_h; (b) $M_{\min}$ as a function of β for different f; and (c) wave-polarity regimes characterized by $V'''(0)$ in the (q_h, q_c) parameter space, with $V'''(0) < 0$ corresponding to the rarefactive and $V'''(0) > 0$ to the compressive regime.

Thus, ion-acoustic solitary structures exist within the Mach number range $M_{\min} < M < M_{\max}$, where $M_{\max}$ is determined by the limiting condition at which the Sagdeev pseudopotential ceases to possess an admissible non-trivial root, i.e., $V(\phi_m, M_{\max}) = 0$. The corresponding solitary-wave profile $\phi(\zeta)$ and electric field $E(\zeta) = -d\phi/d\zeta$ are obtained by numerically integrating Eq. (4).

In order to map the precise boundaries required for the existence of conventional solitary waves, we first explore the behavior of $M_{\min}$ with the non-extensive parameters (q_c, q_h) , temperature ratio (β) and cold electron fraction (f), which are shown in the Fig. 1(a) and 1(b) respectively. Specifically Fig. 1(a) is plotted as $M_{\min}$ vs q_c for different q_h and the Fig. 1(b) is plotted to see the variation of $M_{\min}$ for different value of β with different f values. It is observed from the Fig. 1(a) that as the non-extensive parameters (both q_c and q_h) increases, the M_{min} decreases which is supported by the Refs. [8,9,29,30]. In Fig. 1(b) as β increases, M_{min} decreases which means at higher value of β the wave can exist in a lower Mach number and as the cold electron

concentration increases, the M_{min} decreases which is also demonstrated similarly in the Refs. [29,30]. Rather than examining the dependence of $M_{\max}$ on the plasma parameters in the same manner as $M_{\min}$, we determine $M_{\max}$ numerically for the selected parameters value. This allows us to verify that the Mach number obtained for the selected parameter values lies within the physically valid Mach number regime, as illustrated in Fig. 2(a) (dash dotted vertical line). Now to investigate the polarity of the emerged solitary structures, the third derivative of the Sagdeev pseudopotential is evaluated at the origin, $\phi = 0$, which is found as:

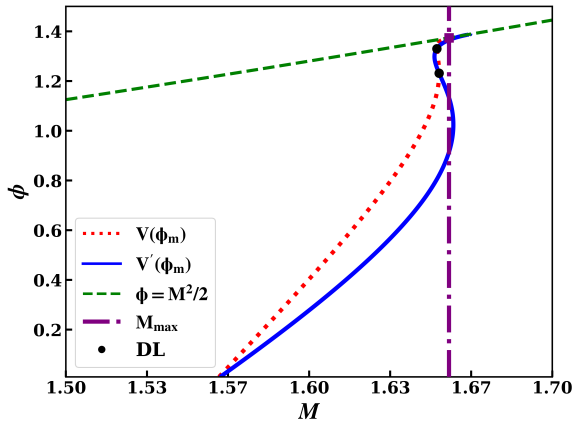
$$V'''(0) = \frac{3}{M_{\min}^4} - f\frac{(q_c+1)(3-q_c)}{4} - (1-f)\beta^2\frac{(q_h+1)(3-q_h)}{4}. \tag{7}$$

The curve $V'''(0) = 0$ marks the existence boundary between different solitary waves. Polarity nature of the waves are dictated by the sign of $V'''(0)$. Specifically the regions inside and outside the curves, corresponding to $V'''(0) < 0$ and $V'''(0) > 0$, respectively, support the rarefactive and compressive solitary waves. These regions are depicted in the (q_h, q_c) parameter plane for some fixed combinations of β and f, as illustrated in Fig. 1(c).

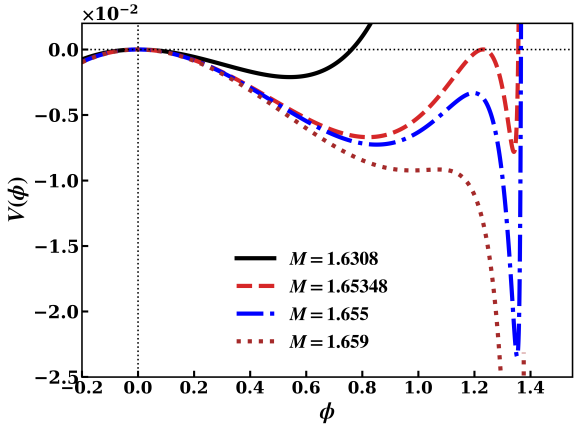
In this study, instead of conventional static parameter boundary plots (e.g., f versus q or β) for determining the critical parameter values, we use the theoretical existence conditions of the solitary structures as depicted in Fig. 2(a). Furthermore, the formation of these localized structures including solitons, double layers, and supersolitons of both polarities are verified topologically using phase portraits (ϕ versus $d\phi/d\zeta$), alongside electric field and potential profiles. These geometric visualizations provide mathematical confirmation of the structures existence and distinct spatial features. Based on this topological framework, the following section presents the numerical analysis used to identify conventional solitary structures.

3 Analysis of double layers and beyond

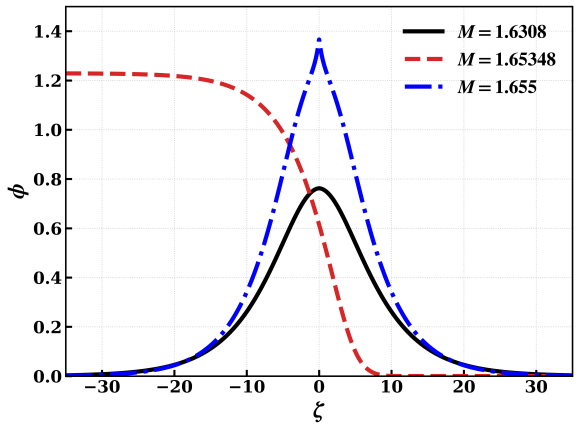
As the double layer represents the lower limiting state of supersoliton and upper limiting state of regular soliton [9,10,29], so if we can find the double layer then it will be easy to check whether our system supports the supersolitons or not. To find the parameter window for the existence of double layers, first we have plotted the Sagdeev pseudopotential $V(M, \phi)$ (red dotted curve) and its first derivative $V'(M, \phi)$ (solid blue curve) in the (M, ϕ) parameter space as depicted in Fig. 2(a) for some fixed parameters $f = 0.31$, $\beta = 0.35024$, which are nearly same ranges as in Refs. [11,29,30,35]. We choose $q_c = 0.28$ and $q_h = 0.75$ ($V''' > 0$ region in Fig. 1(c)) for possible compressive waves ($\phi > 0$). Our parameter investigation reveals two intersection points (M, ϕ): $(1.65348, 1.2313)$ and $(1.6525, 1.3299)$ satisfying the conditions $V(\phi_{DL}) = 0$ and $V'(\phi_{DL}) = 0$. Upon further analysis, the point $(1.6525, 1.3299)$ does not satisfy the complete set of conditions for double layer formation because it gives $V(M_{DL}, \phi_{DL}) > 0$. The violet dash-dotted vertical line represents the upper Mach number limit (M_{max}), beyond which no solitary structures are found for the chosen parameters value. Additionally, the green dashed curve denotes the maximum allowable amplitude limit, defined by $\phi_{max} = M^2/2$ for the for compressive waves, which validates Eq. (3). As required, our confirmed double layer solution at $(1.65348, 1.2313)$ correctly lies within ϕ_{max} and M_{max}. The corresponding pseudo-potential profile for this double layer is plotted in Fig. 2(b) depicted with red dashed curve at the Mach number $M_{DL} = 1.65348$, which is considered as the upper limit of Mach number of regular solitons, because regular soliton exists in the Mach number regime $M_{\min} < M < M_{DL}$ in most



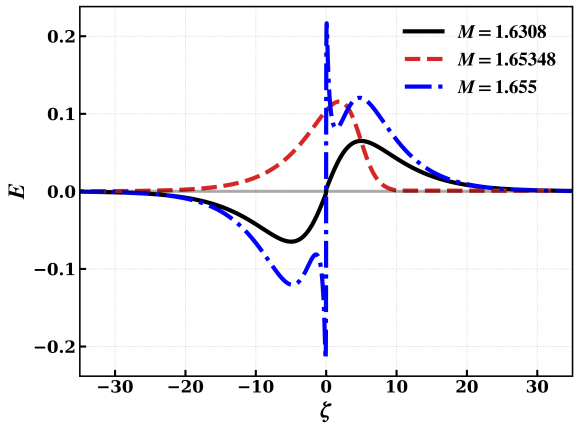
(a)



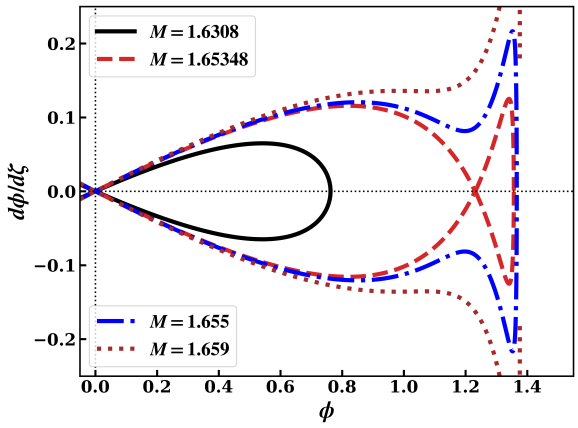
(b)



(c)



(d)



(e)

Figure 2: Characteristics of compressive waves: (a) plot of $V(\phi)$ and $V'(\phi)$ in (M, ϕ) plane; (b) ϕ versus $V(\phi)$; (c) solitary wave profile (ϕ versus ζ); (d) electric field versus transformed spatial variable ζ; and (e) phase portraits of the corresponding structures. The parameters $f = 0.31$, $\beta = 0.35024$, $q_c = 0.28$, and $q_h = 0.75$ are fixed, while the Mach number M is varied as $M = 1.6308$ (solid black), $M = 1.65348$ (red dashed), $M = 1.655$ (blue dash-dotted), and $M = 1.659$ (brown dotted).

of the cases. On further increasing the Mach number ($M > M_{DL}$), interestingly the curve with $M = 1.655$ (blue dashed dotted) generates three local extrema or two distinct wells which is nothing but the signature for the existence of supersoliton. Earlier studies of three component plasmas, considering both unmagnetized [29] and magnetized [30] configurations, have identified the solitary waves and double layers; however, no supersoliton structures were reported in those studies. In our analysis it is seen that for Mach numbers M_{ss} beyond the Mach number of double layer i.e, $M_{ss} > M_{DL}$ supersolitons appear. In Fig. 2(b) the pseudo-potential curve obtained with Mach number $M_{ss} = 1.655$ (blue dashed dotted) with two wells clearly confirms the supersoliton structure, which is not reported in Ref. [29].

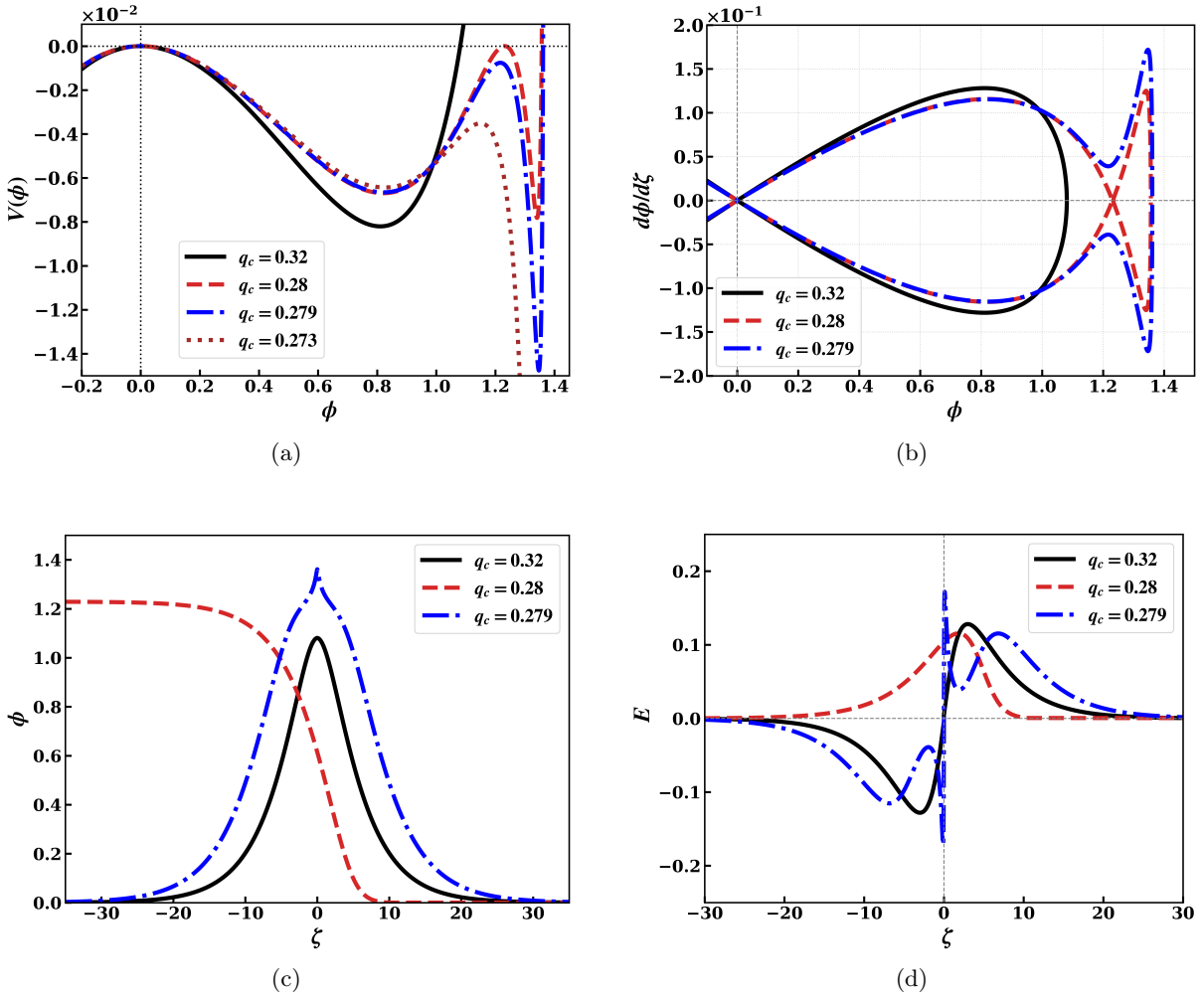


Figure 3: (a) ϕ versus $V(\phi)$; (b) phase portrait (ϕ versus $d\phi/d\zeta$); (c) solitary-wave profile ϕ versus ζ; and (d) electrostatic field for fixed $M = 1.65348$, $\beta = 0.35024$, and $f = 0.31$, for different values of q_c: $q_c = 0.32$ (solid black), $q_c = 0.28$ (red dashed) and $q_c = 0.279$ (blue dash-dotted).

In addition, the presence of the supersoliton can be further verified through the electric field signature and phase portrait diagram, as depicted in Fig. 2(d) and (e) respectively. The phase portrait of a regular soliton forms a standard closed loop around the equilibrium points ($\phi = 0$ and $\phi = \phi_m$), whereas a double layer exhibits a step-like potential with a non-returning separatrix trajectory connecting distinct asymptotic states, as shown in the solitary wave profile in Fig. 2(c), corresponding to a heteroclinic orbit in the phase portrait shown in Fig. 2(e). The supersoliton is distinctly identified by a tri-polar electric field signature with characteristic wiggles on its wings

as seen in Fig. 2(d) and a phase trajectory that wraps completely around an internal separatrix, displaying pinch-like oscillations as in Fig. 2(e). Upon further increasing the Mach number to $M = 1.659$, i.e., $M > M_{ss}$, the solution ceases to represent an ordinary solitary wave, as the Sagdeev pseudopotential well does not return to equilibrium point of electrostatic potential (ϕ). Consequently, the corresponding ion density [Eq. (3)] becomes unphysical, rendering the solitary wave solution physically inadmissible. In conclusion, beyond the compressive supersoliton regime, i.e., for $M \geq 1.659$, no regular solitons, double layers, supersolitons, or other standard nonlinear structures are found. This result leads that the nonlinear structures are highly sensitive to the Mach number and exist only within a narrow Mach-number regime, as discussed above.

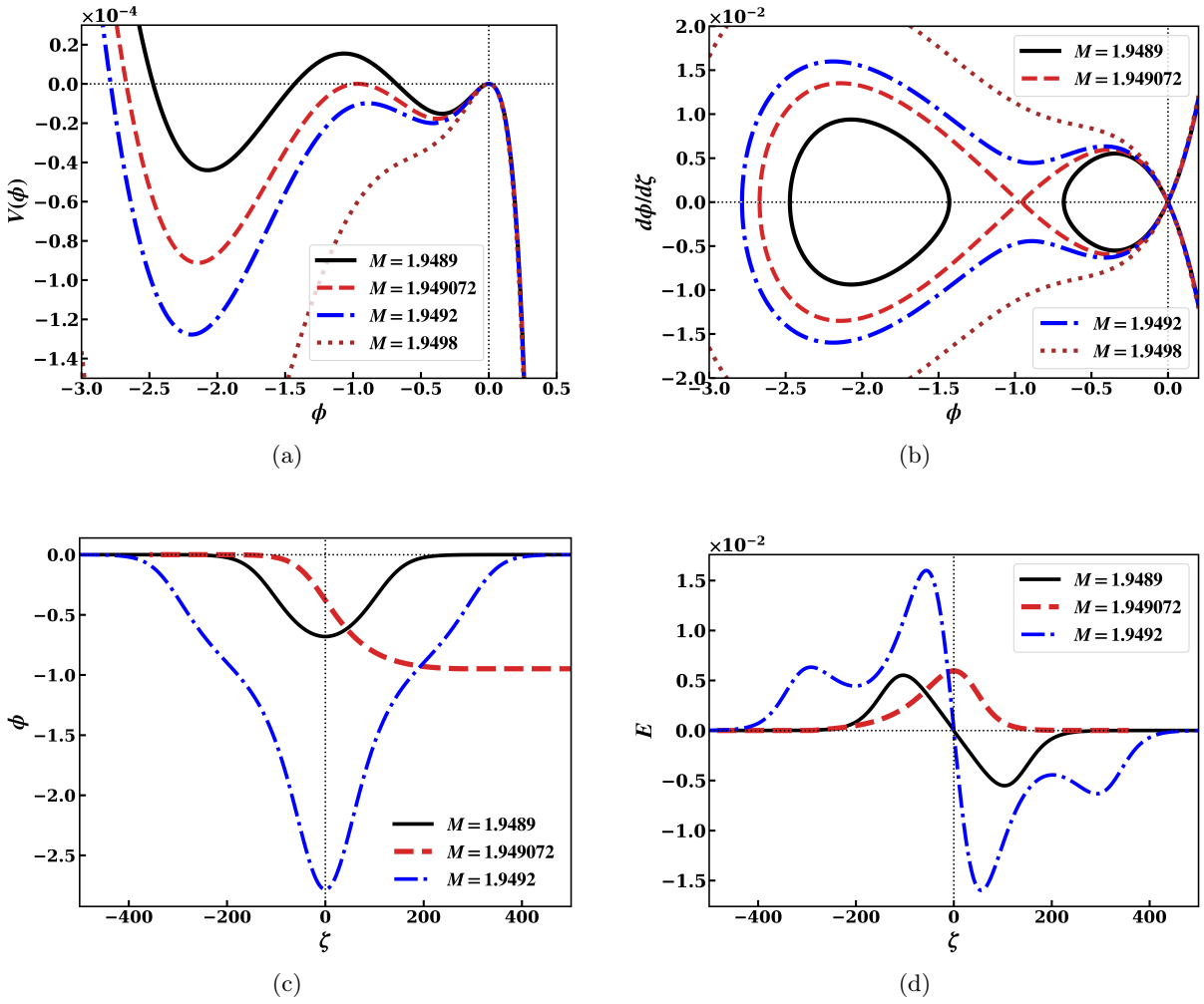


Figure 4: (a) ϕ versus $V(\phi)$; (b) phase portrait; (c) solitary-wave profile; and (d) electrostatic field for fixed $q_h = 0.3055$, $q_c = -0.729$, $f = 0.31$, and $\beta = 0.4944$, for different values of Mach number M: $M = 1.9489$ (solid black), $M = 1.949072$ (red dashed), $M = 1.9492$ (blue dash-dotted) and $M = 1.9498$ (brown dotted).

To examine the effect of the non-extensive parameter q_c on these generated compressive waves, Sagdeev pseudopotential $V(\phi)$ is plotted in Fig. 3 as a function of the electrostatic potential ϕ for different values of q_c, with the Mach number fixed at $M = 1.65348$ and all other plasma parameters kept identical to those considered in Fig. 2. At $q_c = 0.32$ (black solid curve), the pseudo-potential exhibits a single well, indicating the formation of a regular soliton, a slight decrease in non-extensive parameter to $q_c = 0.28$ (red dashed curve) yields a double layer structure. Upon further decreasing q_c to 0.279 (blue dash-dotted curve) the two wells emerge, forming a

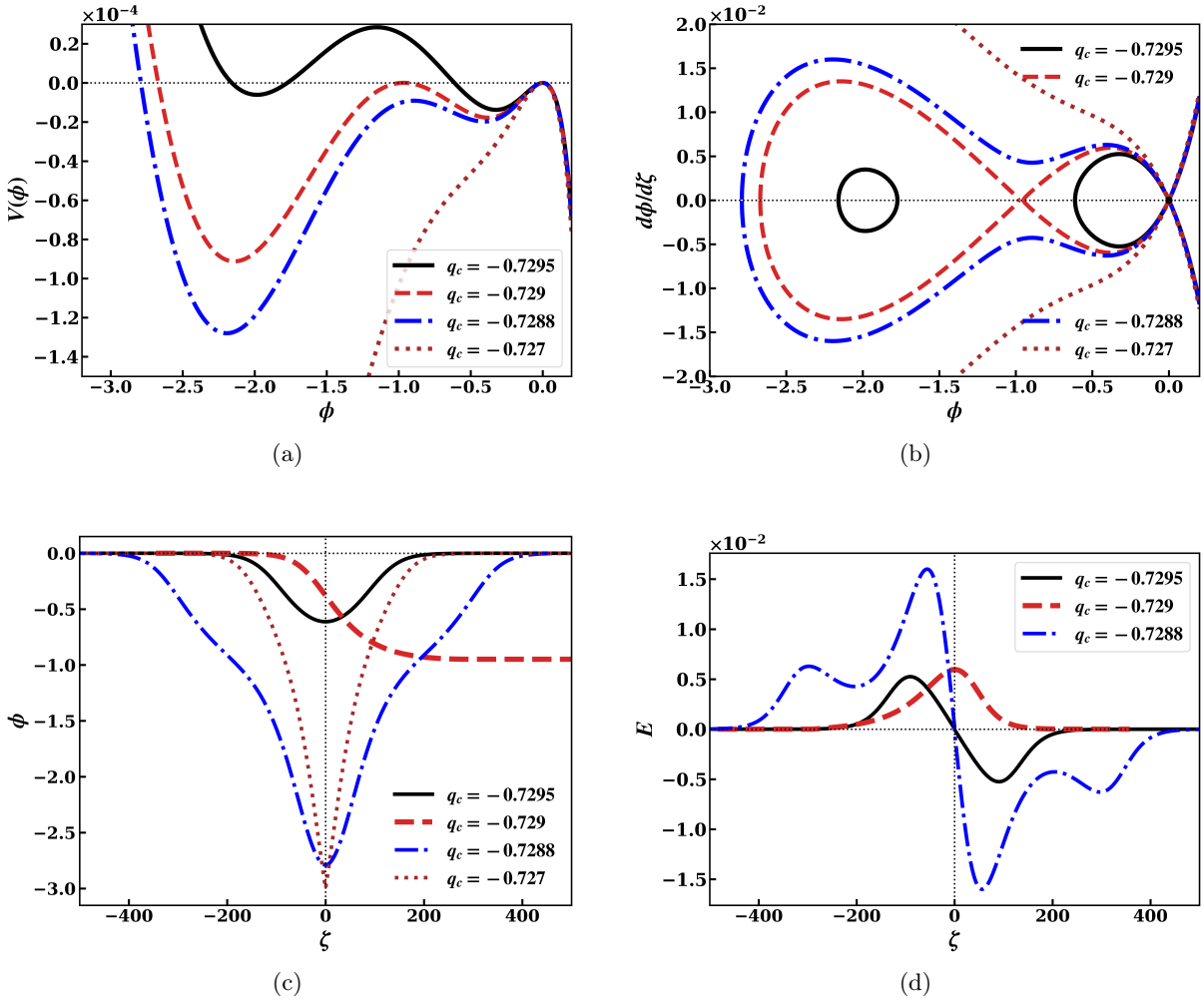


Figure 5: (a) ϕ versus $V(\phi)$; (b) phase portrait; (c) solitary-wave profile; and (d) electrostatic field for fixed $q_h = 0.3055$, $f = 0.31$, $M = 1.949072$, and $\beta = 0.4944$, for different values of q_c: $q_c = -0.7295$ (solid black), $q_c = -0.729$ (red dashed), $q_c = -0.7288$ (blue dash-dotted) and $q_c = -0.727$ (brown dotted).

supersoliton with larger amplitude than DL as demonstrated in Fig. 3(a). The corresponding phase portraits, solitary wave profiles, and spatial electric field signatures for these emergent structures are plotted in Figs. 3(b), 3(c) and 3(d) respectively. On decreasing beyond the supersoliton q_c limit there is solitary wave generated. Ultimately, these results demonstrate the significant influence of the non-extensive parameter, as small changes in electron non-extensivity can substantially modify the characteristics and amplitude of the nonlinear structures, allowing one type of structure to transform into another.

Again for investigating rarefactive wave formation, the non-extensive parameters $q_h = 0.3055$ and $q_c = -0.729$ are selected from the relevant region of Fig. 1(c), where $V''' < 0$ for $f = 0.31$ and $\beta = 0.4944$. With these parameters the Sagdeev potential profiles are plotted for different Mach numbers in Fig. 4(a), which clearly shows the nonlinear waves in the negative electrostatic potential region ($\phi < 0$). Interestingly, all three nonlinear structures are obtained again, similar to the compressive case. Tribeche et al. [34] successfully investigated solitary waves and reported the existence of rarefactive nonlinear solitary structures for negative non-extensive parameter values in the range of -0.78 to -0.7 at a Mach number of $M = 3.2$, which is consistent with our findings for such negative non-extensive parameter values. For $M = 1.9489$ (solid black curve),

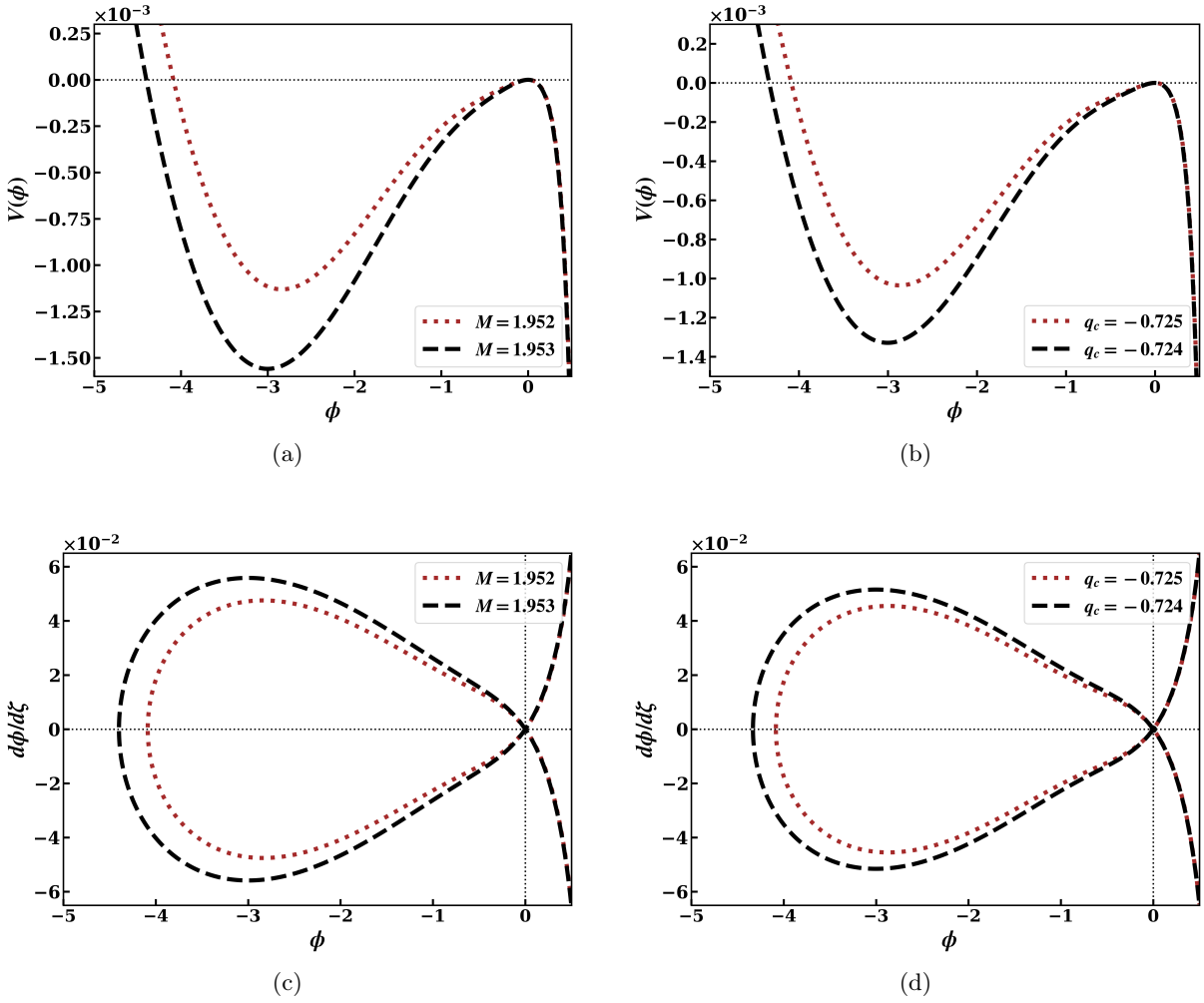


Figure 6: Solitary structures beyond the supersoliton limit in the rarefactive regime: (a) Sagdeev pseudo-potential $V(\phi)$ versus ϕ for $M = 1.952$ (brown dotted) and $M = 1.953$ (black dashed); (b) $V(\phi)$ versus ϕ for $q_c = -0.725$ (brown dotted) and $q_c = -0.724$ (black dashed); (c) and (d) corresponding phase portraits. The remaining parameters are fixed at the values used in Fig. 5.

the pseudopotential exhibits well defined roots at non-zero values of ϕ, satisfying the standard conditions for rarefactive soliton. As the Mach number is increased to 1.949072 (dashed red curve), a double layer emerges. This is confirmed by the Sagdeev pseudopotential curve, which becomes tangent to the horizontal axis at a specific negative potential (ϕ_{DL}) satisfying all the conditions stated above for double layer, which is not reported in three component plasma of Ref. [15]. With $M = 1.9492$ (blue dash dotted), the Sagdeev pseudo-potential profile gives two sub wells, indicating the existence of rarefactive supersoliton, which is not found in Refs. [16,29,30] on varying Mach numbers. The corresponding phase portrait, electrostatic potential profile and electrostatic field profiles are plotted in Figs. 4(b), 4(c) and 4(d) respectively for further justifying the emergent solitary structures . On further increasing the Mach number (1.9498), the two distinct wells of the Sagdeev pseudopotential gradually merge, and the supersoliton evolves into a regular soliton with increasing amplitude. This transition is further examined in detail in Fig. 6. Further in Fig. 5 the effect of the non-extensive parameter on the rarefactive waves are investigated for different values of q_c, while q_h, M, β, and f are kept fixed at the values considered in Fig. 4. Here, Fig. 5(a) shows the pseudopotential profiles for some distinct values of q_c; at $q_c = -0.7295$ (solid black curve), a rarefactive solitary wave is formed, while at

$q_c = -0.729$ (dashed red curve) a double-layer and at $q_c = -0.7288$ (blue dashed-dotted curve) a supersoliton is observed. Figs 5(b), 5(c), and 5(d) present the corresponding phase portraits, potentials and electric field characteristics, providing confirmation of the identified rarefactive structures. Further if we consider $q_c = -0.727$ the sub wells in the supersoliton disappeared and return to a regular solitary structure with larger amplitude than the supersoliton. Although both q_c and q_h characterize the non-extensivity of their respective plasma components, this controlled analysis isolates the individual contribution of q_c, while q_h remains constant within the physically admissible regime. Therefore, the effect of q_c on the evolution of rarefactive structures can be clearly identified. The behavior of these electrostatic waves can also be studied by varying q_h, as its influence on the wave dynamics with Mach number is already seen in Fig. 1(a)

The evolution of rarefactive waves, analyzed through varying Mach numbers (Fig. 4) and non-extensive parameters (Fig. 5), reveals a distinct transition sequence from a supersoliton to a regular solitary wave regime. This transition is verified by plotting both the Sagdeev potential profiles (Figs. 6(a) and (b)) and the corresponding phase portraits (Figs. 6(c) and (d)) for specific parameters, such as $M = 1.952$ and $q_c = -0.725$ which are beyond the supersoliton Mach number and non-extensivity limit, while keeping the remaining parameters fixed as studied in Fig. 4 and Fig. 5 respectively. The Sagdeev potential displays a single well without any internal subwells in both cases, indicating that the waves have lost its supersoliton characteristics and transit into a regular soliton with a higher amplitude. Furthermore, the phase portraits lack the pinched structures typical of supersolitons, instead exhibiting closed trajectories that definitively confirm the shift to a rarefactive regular solitons. These results are distinct from earlier works in three component, unmagnetized collisionless two temperature electron plasma.

4 Conclusions

In this work, we have investigated the finite amplitude ion-acoustic solitary structures in a three component unmagnetized, collisionless plasma composed of cold fluid positive ions and two temperature (cold and hot) electrons featuring with independent non-extensive parameters (q_c and q_h). The wave characteristics are systematically studied by examining how the properties and nature of the solitary structures vary with changes in the relevant plasma parameters. The polarity regimes of these structures are then identified by analyzing the corresponding parameter dependencies, which provides the permissible conditions for the existence of compressive and rarefactive waves. The analysis reveals the occurrence of solitons, double layers and supersolitons for different plasma parameters. The significant investigated findings of this present work are summarized as follows: The existence of ion-acoustic compressive solitons, double layers and supersolitons are studied for distinct Mach numbers and non-extensive parameter values. The waves amplitude exhibits strong dependence on these parameters as, increasing Mach number, the amplitude is found to increase, whereas a decrease in the non-extensive parameter (q_c) leads to an enhancement of the amplitude up to a critical limit, beyond which no solitary wave solution exists. Thus, the compressive waves characteristics are strongly governed by the Mach number (M) and non-extensive parameter (q_c). The system also supports rarefactive waves, whose amplitude is observed very sensitive to the Mach number and the magnitude of q_c. Earlier studies [29] reported the existence of solitons and double layers only, while our parametric investigation gives a much richer spectrum of nonlinear wave structures. Most notably, in this work solitons, double layers and supersolitons of both polarities are observed, which is unique in three compo-

nent plasma configuration. Hence, the emergence of these structures is highly sensitive to the parameters variation. Another important findings of this study is the wave transition exhibited in the rarefactive regime when the Mach number increases beyond the existence of supersoliton. The structure no longer persists as a supersoliton; rather, it transits into a regular soliton with higher amplitude (Fig. 6(a)), following the sequence: soliton (before the double layer) →double layer → supersoliton → soliton (after the supersoliton). A similar transition is also observed with the changes in the non-extensive parameter q_c (Fig. 6(b)), indicating that the existence regime of supersoliton is narrow and highly constrained. Hence, this transition can occur either through Mach number or through the degree of non-extensivity, showing that the rarefactive supersolitons as an intermediate solitary wave states. These findings are unique compared to earlier studies in similar three component plasmas [29,30,32]. Hence, the parametric investigation in this work reveals solitons, double layers and supersolitons of both polarities along with clear transitions among these nonlinear structures, providing a better understanding of their formation and evolution. This approach may help interpret the physical significance of nonlinear electrostatic structures observed in space, astrophysical, and laboratory plasmas, thereby providing a theoretical framework for understanding future observations involving two-temperature non-Maxwellian electron populations.

Author declarations

Conflict of Interest

The authors have no conflicts to disclose.

Funding

No funding was received from any funding organization for the research, authorship, or publication of this article.

Author Contributions

Somir Ali: Investigation (equal); Formal analysis (equal); Methodology (equal); Writing original draft.
K. Saharia: Supervision; Conceptualization (equal); Writing–review and editing (equal).

Data availability

The data that support the findings of this study are available within the article.

References

[1] Dubinov, A. E., & Kolotkov, D. Yu. (2012). Ion-Acoustic Super Solitary Waves in Dusty Multispecies Plasmas. IEEE Transactions on Plasma Science, 40(5), 1429–1433. https://doi.org/10.1109/tps.2012.2189026

[2] Dubinov, A. E., Kolotkov, D. Yu., & Sazonkin, M. A. (2012). Supernonlinear Waves in Plasma. Plasma Physics Reports, 38(10), 833–844. https://doi.org/10.1134/s1063780x12090036

[3] Dubinov, A. E., & Kolotkov, D. Yu. (2012). Ion-acoustic supersolitons in plasma. Plasma Physics Reports, 38(11), 909–912. https://doi.org/10.1134/s1063780x12100054

[4] Baluku, T. K., Hellberg, M. A., & Verheest, F. (2010). New light on ion acoustic solitary waves in a plasma with two-temperature electrons. EPL (Europhysics Letters), 91(1), 15001. https://doi.org/10.1209/0295-5075/91/15001

[5] DAS, A., BANDYOPADHYAY, A., & DAS, K. P. (2012). An analytical study on the existence of solitary structure at $M = M_c$. Journal of Plasma Physics, 78(5), 565–584. https://doi.org/10.1017/s0022377812000372

[6] Verheest, F. (2009). Nonlinear acoustic waves in nonthermal plasmas with negative and positive dust. Physics of Plasmas, 16(1). https://doi.org/10.1063/1.3059411

[7] Verheest, F. (2011). Dust-acoustic solitary modes in plasmas with isothermal and non-thermal ions: Polarity switches and coexistence domains. Physics of Plasmas, 18(8). https://doi.org/10.1063/1.3610560.

[8] Sahu, B. (2011). Ion acoustic solitary waves and double layers with nonextensive electrons and thermal positrons. Physics of Plasmas, 18(8). https://doi.org/10.1063/1.3620413

[9] El-Wakil, S. A., Abulwafa, E. M., & Elhanbaly, A. A. (2017). Super-soliton dust-acoustic waves in four-component dusty plasma using non-extensive electrons and ions distributions. Physics of Plasmas, 24(7). https://doi.org/10.1063/1.4991406

[10] Baghel, J., Singh, K., & Kumar, K. (2025). Electrostatic supersolitons, flat-top solitons, and double layers in a warm multicomponent plasma with two-temperature electrons. Physics of Plasmas, 32(9). https://doi.org/10.1063/5.0283744

[11] Verheest, F., Hellberg, M. A., & Kourakis, I. (2013). Electrostatic supersolitons in three-species plasmas. Physics of Plasmas, 20(1). https://doi.org/10.1063/1.4775085

[12] Singh, S. V., & Lakhina, G. S. (2015). Ion-acoustic supersolitons in the presence of non-thermal electrons. Communications in Nonlinear Science and Numerical Simulation, 23(1-3), 274–281. https://doi.org/10.1016/j.cnsns.2014.11.017

[13] Mushinzimana, X., Nsengiyumva, F., & Yadav, L. L. (2021). Large amplitude slow ion-acoustic solitons, supersolitons, and double layers in a warm negative ion plasma with superthermal electrons. AIP Advances, 11(2). https://doi.org/10.1063/5.0039372

[14] Rufai, O. R., Bharuthram, R., Singh, S. V., & Lakhina, G. S. (2014). Ion acoustic solitons and supersolitons in a magnetized plasma with nonthermal hot electrons and Boltzmann cool electrons. Physics of Plasmas, 21(8). https://doi.org/10.1063/1.4891877

[15] Debnath, D., Bandyopadhyay, A., & Das, K. P. (2018). Ion acoustic solitary structures in a magnetized nonthermal dusty plasma. Physics of Plasmas, 25(3). https://doi.org/10.1063/1.5021127

[16] Paul, A., Bandyopadhyay, A., & Das, K. P. (2017). Dust ion acoustic solitary structures in presence of nonthermally distributed electrons and positrons. Physics of Plasmas, 24(1). https://doi.org/10.1063/1.4975089

[17] Lakhina, G. S., Singh, S. V., & Kakad, A. P. (2014). Ion acoustic solitons/double layers in two-ion plasma revisited. Physics of Plasmas, 21(6). https://doi.org/10.1063/1.4884791

[18] Verheest, F., Lakhina, G. S., & Hellberg, M. A. (2014). No electrostatic supersolitons in two-component plasmas. Physics of Plasmas, 21(6). https://doi.org/10.1063/1.4881471

[19] Dovner, P. O., Eriksson, A. I., Boström, R., & Holback, B. (1994). Freja multiprobe observations of electrostatic solitary structures. Geophysical Research Letters, 21(17), 1827–1830. Portico. https://doi.org/10.1029/94gl00886

[20] Boström, R., Gustafsson, G., Holback, B., Holmgren, G., Koskinen, H., & Kintner, P. (1988). Characteristics of Solitary Waves and Weak Double Layers in the Magnetospheric Plasma. Physical Review Letters, 61(1), 82–85. https://doi.org/10.1103/physrevlett.61.82

[21] Matsumoto, H., Kojima, H., Miyatake, T., Omura, Y., Okada, M., Nagano, I., & Tsutsui, M. (1994). Electrostatic solitary waves (ESW) in the magnetotail: BEN wave forms observed by GEOTAIL. Geophysical Research Letters, 21(25), 2915–2918. Portico. https://doi.org/10.1029/94gl01284

[22] McFadden, J. P., Carlson, C. W., Ergun, R. E., Mozer, F. S., Muschietti, L., Roth, I., & Moebius, E. (2003). FAST observations of ion solitary waves. Journal of Geophysical Research: Space Physics, 108(A4). Portico. https://doi.org/10.1029/2002ja009485

[23] Cattell, C. A., Dombeck, J., Wygant, J. R., Hudson, M. K., Mozer, F. S., Temerin, M. A., Peterson, W. K., Kletzing, C. A., Russell, C. T., & Pfaff, R. F. (1999). Comparisons of Polar satellite observations of solitary wave velocities in the plasma sheet boundary and the high altitude cusp to those in the auroral zone. Geophysical Research Letters, 26(3), 425–428. Portico. https://doi.org/10.1029/1998gl900304

[24] Shi, P., Srivastav, P., Barbhuiya, M. H., Cassak, P. A., Scime, E. E., & Swisdak, M. (2022). Laboratory Observations of Electron Heating and Non-Maxwellian Distributions at the Kinetic Scale during Electron-Only Magnetic Reconnection. Physical Review Letters, 128(2). https://doi.org/10.1103/physrevlett.128.025002

[25] Ergun, R. E., Carlson, C. W., McFadden, J. P., Mozer, F. S., Delory, G. T., Peria, W., Chaston, C. C., Temerin, M., Elphic, R., Strangeway, R., Pfaff, R., Cattell, C. A., Klumpar, D., Shelley, E., Peterson, W., Moebius, E., & Kistler, L. (1998). FAST satellite wave observations in the AKR source region. Geophysical Research Letters, 25(12), 2061–2064. Portico. https://doi.org/10.1029/98gl00570

[26] Pottelette, R., Ergun, R. E., Treumann, R. A., Berthomier, M., Carlson, C. W., McFadden, J. P., & Roth, I. (1999). Modulated electron-acoustic waves in auroral density cavities: FAST observations. Geophysical Research Letters, 26(16), 2629–2632. Portico. https://doi.org/10.1029/1999gl900462

[27] Tsallis, C. (1988). Possible generalization of Boltzmann-Gibbs statistics. Journal of Statistical Physics, 52(1-2), 479–487. https://doi.org/10.1007/bf01016429

[28] Gupta, H. M., Campanha, J. R., & Schinaider, S. J. (2008). Size limiting in Tsallis statistics. Physica A: Statistical Mechanics and Its Applications, 387(27), 6745–6751. https://doi.org/10.1016/j.physa.2008.09.009

[29] Shalini, & Saini, N. S. (2014). Ion acoustic solitary waves and double layers in a plasma with two temperature electrons featuring Tsallis distribution. Physics of Plasmas, 21(10). https://doi.org/10.1063/1.4897177

[30] Hatami, M. M. (2025). Investigation of ion acoustic double layers in magnetized plasma with two nonextensive electron species. Scientific Reports, 16(1). https://doi.org/10.1038/s41598-025-31448-6

[31] Singla, A., Singla, S., Saini, N. S., & Gill, F. S. (2024). Ion-acoustic solitons in multicomponent plasma with two temperature non-Maxwellian electrons. Radiation Effects and Defects in Solids, 180(3-4), 476–488. https://doi.org/10.1080/10420150.2024.2381237

[32] Kakoti, R., & Saharia, K. (2020). Effect of nonextensivity on the characteristics of supersolitons in a two-temperature electron plasma. Contributions to Plasma Physics, 60(3). Portico. https://doi.org/10.1002/ctpp.201900167

[33] Dalui, S., Sardar, S., & Bandyopadhyay, A. (2021). Arbitrary amplitude ion acoustic solitons, double layers and supersolitons in a collisionless magnetized plasma consisting of non-thermal and isothermal electrons. Zeitschrift Für Naturforschung A, 76(5), 455–468. https://doi.org/10.1515/zna-2020-0296

[34] Tribeche, M., Djebarni, L., & Amour, R. (2010). Ion-acoustic solitary waves in a plasma with a q-nonextensive electron velocity distribution. Physics of Plasmas, 17(4). https://doi.org/10.1063/1.3374429

[35] Baluku, T. K., & Hellberg, M. A. (2012). Ion acoustic solitons in a plasma with two-temperature kappa-distributed electrons. Physics of Plasmas, 19(1). https://doi.org/10.1063/1.3675866